National Renewable Energy Laboratory
Innovation for Our Energy Future

A national laboratory of the U.S. Department of Energy
Office of Energy Efficiency & Renewable Energy

Thermal Interface Materials for Power Electronics Applications

Preprint

S. Narumanchi, M. Mihalic, and K. Kelly
National Renewable Energy Laboratory

G. Eesley
Delphi Electronics

Presented at Itherm 2008
Orlando, Florida
May 28–31, 2008

Conference Paper
NREL/CP-540-42972
July 2008

NREL is operated by Midwest Research Institute • Battelle Contract No. DE-AC36-99-GO10337

THERMAL INTERFACE MATERIALS FOR POWER ELECTRONICS APPLICATIONS

Sreekant Narumanchi, Mark Mihalic, and Kenneth Kelly
National Renewable Energy Laboratory
1617 Cole Blvd.
Golden, CO 80401-3393, USA
Phone: (303)275-4062
Fax: (303)275-4415
Email: sreekant_narumanchi@nrel.gov

Gary Eesley
MC: D-16, Delphi Electronics
One Corporate Center, 2705 Goyer Rd.
Kokomo, IN 46904-9005, USA

ABSTRACT

In a typical power electronics package, a grease layer forms the interface between the direct bond copper (DBC) layer or a baseplate and the heat sink. This grease layer has the highest thermal resistance of any layer in the package. Reducing the thermal resistance of this thermal interface material (TIM) can help achieve the FreedomCAR partnership goals of using a glycol water mixture at 105°C or even air cooling. It is desirable to keep the maximum temperature of the conventional silicon die below 125°C, trench insulated gate bipolar transistors (IGBTs) below 150°C, and silicon carbide-based devices below 200°C. Using improved thermal interface materials enables the realization of these goals and the dissipation of high heat fluxes. The ability to dissipate high heat fluxes in turn enables a reduction in die size, cost, weight, and volume. This paper describes our progress in characterizing the thermal performance of some conventional and novel thermal interface materials. We acquired, modified, and improved an apparatus based on the ASTM D5470 test method and measured the thermal resistance of various conventional greases. We also measured the performance of select phase-change materials and thermoplastics through the ASTM steady-state and the transient laser flash approaches, and compared the two methodologies. These experimental results for thermal resistance are cast in the context of automotive power electronics cooling. Results from numerical finite element modeling indicate that the thermal resistance of the TIM layer has a dramatic effect on the maximum temperature in the IGBT package.

KEY WORDS: Thermal resistance, steady state, transient, modeling, greases, PCMs, IGBTs, ASTM D5470, laser flash

NOMENCLATURE

A	area, mm^2
APEEM	Advanced Power Electronics and Electrical Machines
ASTM	American Society of Testing and Materials
BLT	bond line thickness, mm, µm
C	specific heat, J/kgK
CNTs	carbon nanotubes
DBC	direct bond copper
IGBT	insulated gate bipolar transistor
k, K	thermal conductivity, W/mK
NIST	National Institute of Standards and Technology
PCM	phase-change materials
Q	heat flow, W
R	thermal resistance/impedance, mm^2K/W
RTD	resistance temperature detector
T	temperature, K, °C
TIM	thermal interface materials

Greek

Δ	difference
ρ	density, kg/m^3

INTRODUCTION

This study falls under the thermal control work being done in the U.S. Department of Energy's (DOE) Advanced Power Electronics and Electrical Machines (APEEM) area, which is part of the broader FreedomCAR and Fuel Partnership in the DOE Vehicle Technologies Program. The National Renewable Energy Laboratory (NREL) leads research and development activities in thermal control related to APEEM activities. The overall objective of these thermal control activities is to develop advanced technologies and effective integrated thermal control systems aimed at meeting the FreedomCAR goals. These goals address key requirements for power electronics, such as target values for the volume, cost, and weight of various subcomponents.

Importance of Thermal Interface Materials

This section demonstrates the importance of thermal interface materials (TIMs) in power electronics applications. Figure 1 shows the different layers constituting a typical insulated gate bipolar transistor (IGBT) package in an inverter. The silicon die is soldered to the direct bond copper (DBC) layer, which is composed of an aluminum nitride layer sandwiched between two copper layers. This DBC layer is soldered to a copper baseplate, and the grease layer serves as the interface between

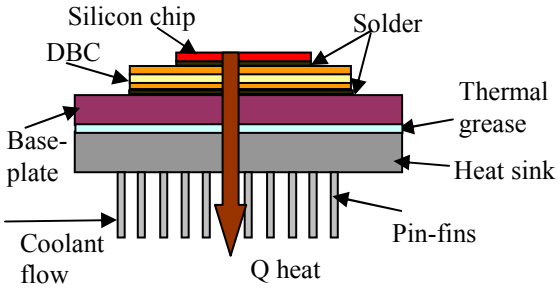

Fig. 1 Layers Constituting the IGBT Package in an Inverter (not to scale)

the baseplate and the heat sink. This thermal grease can be up to 100 microns thick (bond-line thickness, or BLT) and, depending on the formulation, it has a thermal conductivity in the range of 0.4 to 5 W/mK. In an actual IGBT package, overall size, layout and processing can cause the DBC substrate to have a camber of up to 100 microns. This implies that, even though the intent is to keep the BLT to a minimum, the TIMs sometimes fill gaps of 100 microns or greater. In most inverter configurations, a clamping mechanism is used in the package. This results in the TIM being subjected to a pressure of the order of 0.17 to 0.34 MPa. Typically, the inverter has a heat sink in which the coolant flows through pin fins in a channel flow configuration.

To assess the impact of thermal resistance, we performed a 3-D finite element analysis using ANSYS. The domain used for the 3-D simulations of the Toyota Prius inverter is shown in Figure 2. Figure 2(a) shows the actual Prius inverter [1]; Figure 2(b) shows the representation of the inverter in ANSYS; Figure 2(c) shows the simulation domain, which consists of 1 IGBT-diode pair; and Figure 2(d) gives some representative temperature contours in the simulation domain. Making use of symmetry boundary conditions helps to reduce the size of the simulation domain. For the results presented here, 40 W heat dissipation is applied in the diode and 160 W heat dissipation in the IGBT. This translates to a heat flux of 120 W/cm^2 in the IGBT and 95 W/cm^2 in the diode. The area of the IGBT is 134.2 mm^2 (13.7 x 9.8 mm), the area of the diode is 0.42 mm^2 (6.6 x 6.4 mm), the DBC top area is 78.7 mm^2 (32.3 x 24.4 mm), and the heat sink convective area is 1464 mm^2 [2]. A convective heat transfer coefficient of 15,000 W/m^{2}K was imposed on the base of the baseplate, as shown in Figure 2(c). The coolant temperature is 105°C. This represents glycol-water coolant at 105°C, since using glycol-water at 105°C is an important FreedomCAR goal. Table 1 shows the thickness and thermal conductivity of the different layers in the package. The stack-up of the different layers is in accordance with Figure 1.

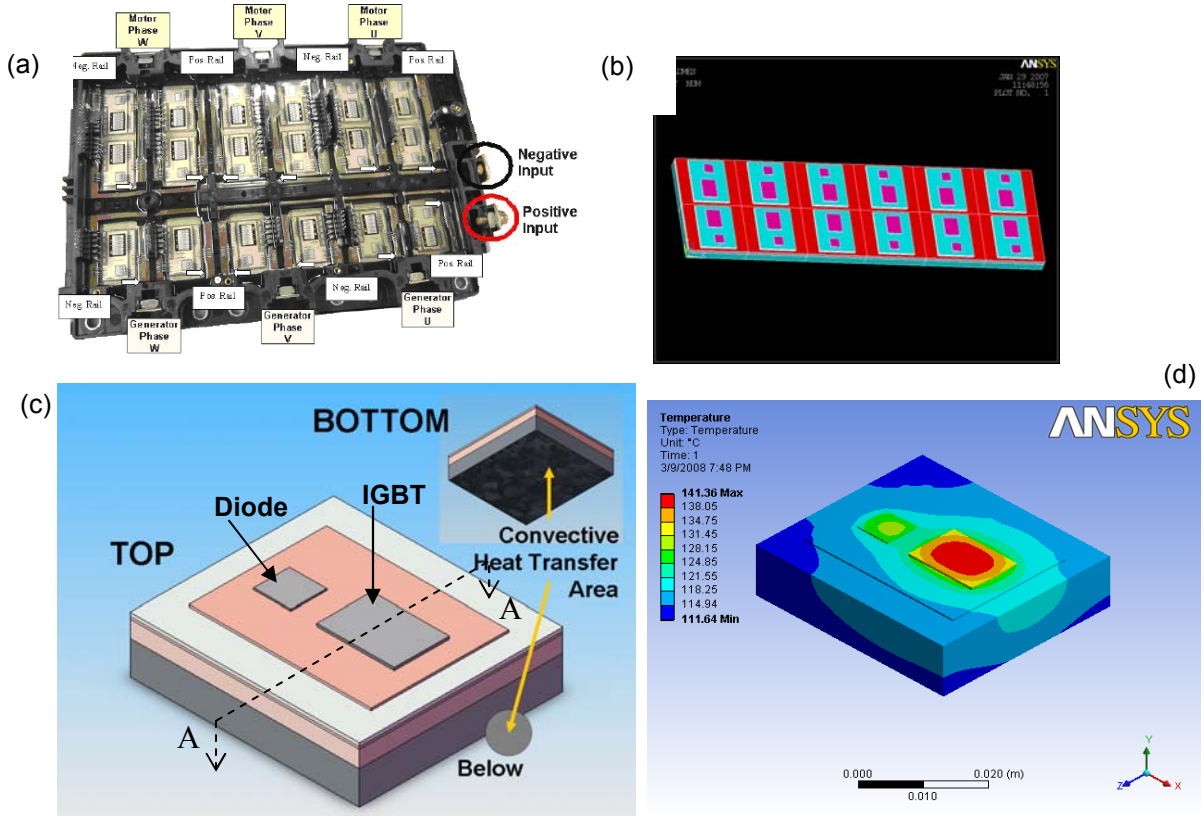

Fig. 2 (a) Prius Inverter [1], (b) Representation of the Prius Inverter in ANSYS, (c) Simulation Domain, (d) Sample Temperature Contours in the Simulation Domain

Table 1. Thickness and Thermal Conductivity of Different Layers in the Package

Material/ Layer	**Thickness** (mm)	**Thermal Conductivity** (W/mK)
Silicon IGBT	0.51	116.0
Silicon diode	0.32	116.0
DBC top copper	0.41	393.0
AlN substrate	0.64	170.0
DBC bottom copper	0.41	393.0
Copper baseplate	3.0	393.0
Aluminum heat sink	6.0	235.0

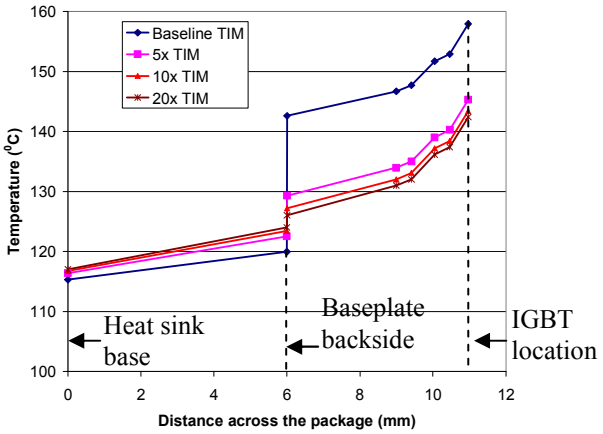

Fig. 3 Impact of TIM Thermal Conductivity on the Maximum Temperature in the Die

Figure 3 shows the impact of the TIM thermal resistance on the maximum die temperature. The baseline case shown corresponds to an average-performance grease, as measured at NREL. For the analysis, the grease thermal resistance was set at 100 mm^2K/W. The 5x TIM case corresponds to a TIM thermal resistance of 20 mm^2K/W (5 times lower than the baseline), the 10x TIM case corresponds to 10 mm^2K/W, and the 20x TIM corresponds to 5 mm^2K/W. Note that the thermal resistance values include the material bulk thermal resistance as well as the contact resistance. The numerical results for temperature are accurate (mesh-independent) to within 1%.

Figure 3 shows that, for the baseline case, there is a significant temperature jump across the TIM (approximately 23°C). For the 5x TIM case, the temperature rise across the TIM is 7°C, for the 10x TIM case, the temperature rise is 4°C, while for the 20x TIM, the temperature rise is only 2°C. Interestingly, reducing the thermal resistance beyond 10x does not significantly change the maximum die temperature. This implies that, once the thermal resistance of the interface material is no longer the dominating resistance (<5 mm^2K/W), it does not matter if its resistance is reduced further. It must be mentioned that these conclusions are dependent upon the package configuration. However, our analysis results for a different package also lead to the conclusion that the TIM stops being a thermal bottleneck below a resistance of 5 mm^2K/W. It is also worth noting that the baseline case corresponds to a TIM thermal resistance of 100 mm^2K/W. It is possible that this resistance could be even higher in an actual inverter, depending on the type and thickness of grease used. Under such conditions, the impact of TIM resistance on the temperature results would be even more dramatic. We will demonstrate this in a subsequent section.

State-of-the-Art of Thermal Interface Materials

In this section, we briefly review the state of the art of thermal interface materials. The total thermal resistance of an interface material is composed of the bulk resistance and the contact resistances. Accordingly, the thermal resistance of an interface material can be written as follows:

$$R = R_c + BLT/k_{TIM}\,, \qquad (1)$$

where R_c is the contact resistance, BLT is the bond-line thickness of the interface material, and k_{TIM} is the bulk thermal conductivity of that material. A high thermal conductivity can reduce the bulk thermal resistance of the interface material, but the contact resistance must also be minimized. Contact resistance is an area that has received significant attention in the literature (e.g., [3-5]).

The focus here is on automotive power electronics cooling, but thermal interface materials play a key role in other microelectronics and high-power applications, as well [5]. The continual increase in cooling demand for microprocessors has led to an increased focus on improving thermal interface materials. Figure 4 shows the state of the art of some thermal interface materials. Significant advances have been made in the development of thermal greases/gels, phase-change materials (PCMs), solders, and carbon nanotubes (CNTs) as interface materials. Greases, gels, and PCMs are the most

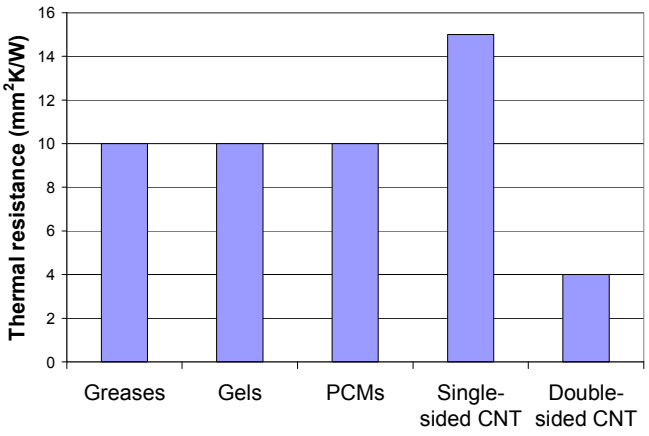

Fig. 4 State-of-the-Art of Some Thermal Interface Materials (CNT: carbon nanotubes, PCMs: phase-change materials; greases, gels, PCMs: [5]; CNTs: [6])

widely used, and their thermal performance has reached 10 mm^2K/W [5]. However, it should be noted that the BLT determines the performance to a significant extent. The high performance of greases/gels and PCMs is for a BLT of less than 25 microns.

In the recent past, significant progress has been made in characterizing the performance of CNTs as TIMs [6]. Figure 4 illustrates that CNTs yield a thermal resistance as low as 4 mm^2K/W [6] under certain conditions.

Challenges for Automotive Power Electronics

Despite the promising performance indicated in Figure 4, a number of barriers have to be overcome before a TIM can be used in automotive power electronics. In the automotive industry, greases are still used predominantly as interface materials. Some problems with greases include pump-out during repeated thermal cycling, dry-out over time [5] (aging effects), and nonuniform application. One reason for their widespread use is that greases fill up the microscopic voids and cavities between mating surfaces very well. This results in a fairly low contact resistance (the first term on the right-hand side in Eq. (1)) at even moderate pressures (lower than 0.2 MPa). We elaborate on this aspect in a subsequent section.

In addition to thermal performance, a TIM should have a long life, be reliable, account for manufacturing variations (e.g., camber in the package of the order of 100 microns), be easy to apply, and be inexpensive. In addition, it is often found that the in situ performance of TIMs is different from the performance during material characterization through one of the several techniques prevailing in the literature. This also brings up the critical issue of the lack of a universally accepted standard for thermal resistance measurements. The ASTM D5470 approach [7] is the closest to being an accepted standard for thermal resistance measurements. However, it has its shortcomings and is not universally accepted.

The several aspects mentioned in the previous paragraphs form the motivation for our research. Typically, in the literature, results for different materials are reported with different techniques. Our intent is to report results for different materials with one single methodology (based on ASTM D5470) and create a consistent, objective database of the thermal performance of materials over different conditions. Our goal is also to understand all the parameters and mechanisms that affect the thermal performance of any TIM. Understanding in situ behavior and the reliability (e.g., impact of thermal cycling, "aging" effects) of TIMs are also important goals. Mechanistic understanding of the thermal degradation of TIMs is currently an open area of research [5]. The ultimate goal of our research is to fabricate/identify a low-thermal-resistance material that would be suitable for automotive power electronics applications.

In this paper, we focus on characterization of the thermal performance of several greases, PCMs and thermoplastics using the ASTM D5470-based steady-state approach. For some select cases (PCMs and thermoplastics), comparisons are also presented between the steady-state approach and the transient laser flash approach. The implications of the results for power electronics package cooling are discussed.

EXPERIMENTS, MODELING, AND DISCUSSION

Test Apparatus for Thermal Resistance Measurements

Steady State. NREL acquired, tested, redesigned, and improved a test stand, based on the ASTM D5470 test method [7, 8], for measuring thermal resistance. The intent of acquiring the test stand was to characterize the thermal performance of novel as well as state-of-the-art thermal interface materials that are suitable for automotive applications and to develop an objective, consistent database.

Figure 5 shows the test apparatus in the Electrical Systems Laboratory at NREL as well as details of the components of the test stand. Figure 5(a) shows the overall test setup; Figure 5(b) shows various components of the apparatus. These include the aluminum hot plate with cartridge heaters embedded in it (Figure 5(c)), the aluminum cold plate with silicone oil circulating through it, the copper spreader blocks, the copper metering blocks, the resistance temperature detectors (RTDs) for accurate temperature measurement, and the pneumatic press for applying load on the sample under test.

Figure 5(c) shows how the different layers stack up. The cylindrical metering blocks are 31.75 mm in diameter and 25.4 mm long. Each metering block has two RTDs, embedded 25.4 mm into the block, for temperature measurement. The metering block is made of oxygen-free copper with a thin nickel coating to prevent oxidation of the copper and also to prevent erosion or corrosion of the block. The average roughness of the surface of the block (facing the TIM) is about 0.5 microns. Surface roughness plays a critical role in determining the contact resistance [5] between the block and the TIM. The dimensions of the square copper spreader blocks are 50.8 x 50.8 mm, the square aluminum hot plate measures 101.6 x 101.6 mm, and the aluminum cold plate measures 152.4 x 88.9 mm.

Load control for the pneumatic press is done via Labview. The required load is set by the user, and a proportional control with a deadband and adaptive gain has been implemented in Labview. The RTD temperatures are also acquired through Labview. The thermal resistance of the sample under test is determined as follows:

$$R = \Delta T\, A_{sample}/Q\,, \tag{2}$$

$$Q = (Q_{top} + Q_{bottom})/2, \tag{3}$$

$$\Delta T = (T_2 - 0.333*(T_1-T_2)) - (T_3 + 0.333*(T_3-T_4)), \tag{4}$$

$$Q_{top} = -k*A_{block}*(T_2 - T_1)/\Delta L, \tag{5}$$

$$Q_{bottom} = -k*A_{block}*(T_4 - T_3)/\Delta L, \tag{6}$$

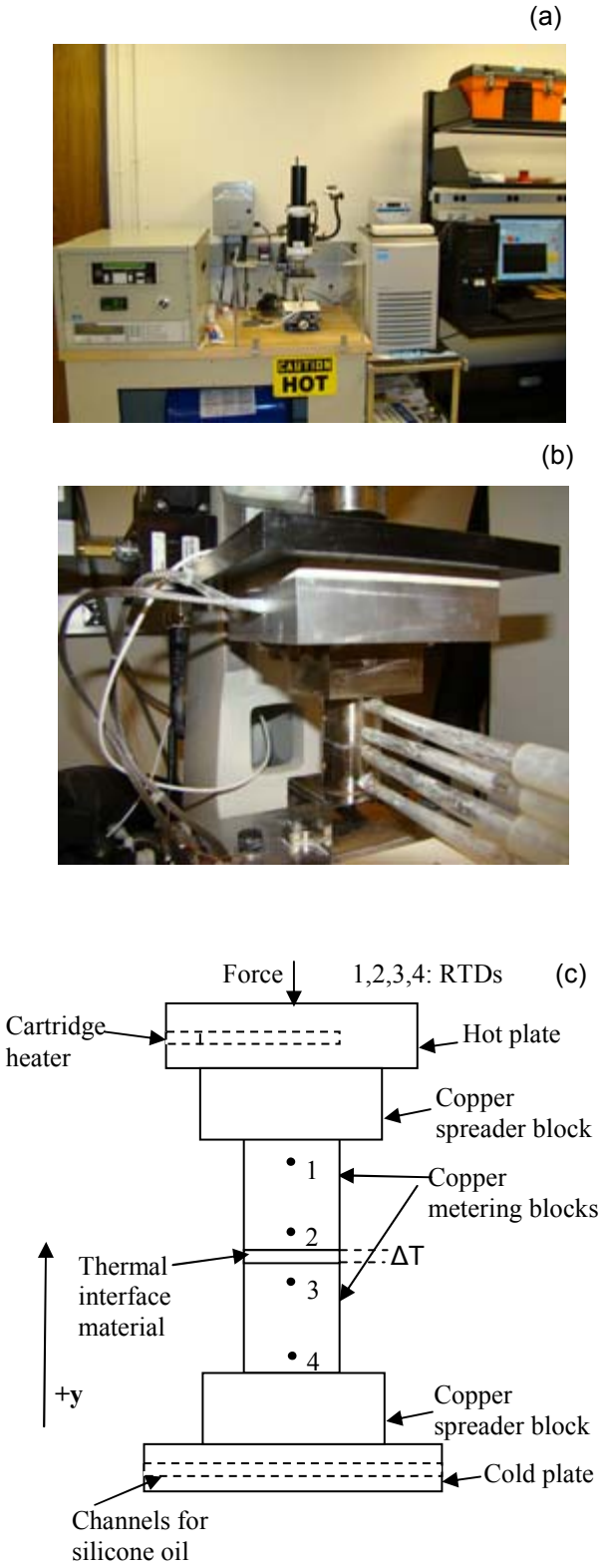

Fig. 5 Test Apparatus for Thermal Resistance Measurements; (a) Facility Setup at NREL, (b) the Apparatus, (c) Stack-up of the Different Layers

where ΔT = the temperature difference across the sample (Figure 5(c)), Q = average power going through the sample, A_{sample} = area of the sample, Q_{top} is the power going through the top metering block (in the –y direction (Figure 5(c)), Q_{bottom} is the power going through the bottom metering block (in the –y direction (Figure 5(c)), k is the thermal conductivity of the oxygen-free copper (393 W/mK), A_{block} is the area of the metering block (791.7 mm^2), T_1, T_2, T_3 and T_4 are the temperatures measured by the RTDs (Figure 5(c)), and ΔL is the distance between RTD probes 1 and 2 (15.24 mm) as well as probes 3 and 4.

Transient. Another method for measuring thermal conductivity is referred to as the transient laser flash method [9]. In this approach, a short laser pulse is used to illuminate the surface of a sample, and the resulting transient temperature rise at the opposite surface is measured as a function of time. Analytic models for this temperature are then fit to the measurement, yielding the thermal diffusivity of the sample,

$$\alpha = K / \rho C_p , \quad (7)$$

where K, ρ, and C_p are the thermal conductivity, density, and specific heat capacity of the material. Independent measurements of ρC_p are used to calculate K from the diffusivity value. This is a somewhat indirect method relative to the steady-state method, but it has the advantage of rapid measurement over a large temperature range.

In most cases of interest for thermal interface materials, we are really more concerned with measuring the total thermal resistance of the TIM sandwiched between substrates of interest. If the TIM-BLT is thermally thin relative to the adjoining substrates, it is possible to determine thermal resistance directly via the transient method [10]. This is based on analytical models derived for laser flash testing of multilayer samples and avoids the need to determine ρC_p.

As more commercially available instrumentation has been developed for this transient method, it is becoming more widely used to characterize TIMs. In addition to the steady-state testing method, we also employed the laser flash method on some of our samples. Our purpose is to validate this technique relative to the steady-state measurement and provide a thorough and consistent evaluation of thermal interface materials. In the test results presented in this paper, the TIM is sandwiched between the DBC aluminum nitride substrate and aluminum. The cross-sectional area of the DBC substrate and aluminum layers are 10 x 10 mm^2. The thickness of the DBC substrate is 1 mm, while the thickness of the aluminum layer is 0.5 mm.

Experimental Uncertainty. The uncertainty in the thermal resistance measured from the steady-state test method (Eq. (2)) was estimated by the method of Kline and McClintock [11]. The accuracy of this methodology is dependent upon the temperature and heat flow in the metering blocks being one-dimensional. For most of the measurements, the discrepancy between the heat flux in the hot and cold metering blocks (Equations 5 and 6) was less than 4%. The accuracy of the RTD probes, during the initial calibration, with respect to a NIST-traceable probe was within 0.04 K. Some drift in the accuracy is possible but is difficult to estimate. The overall

uncertainty in the resistance measurements is estimated to be ±10% (at 95% confidence levels). The repeatability of the experimental results was within ±4%.

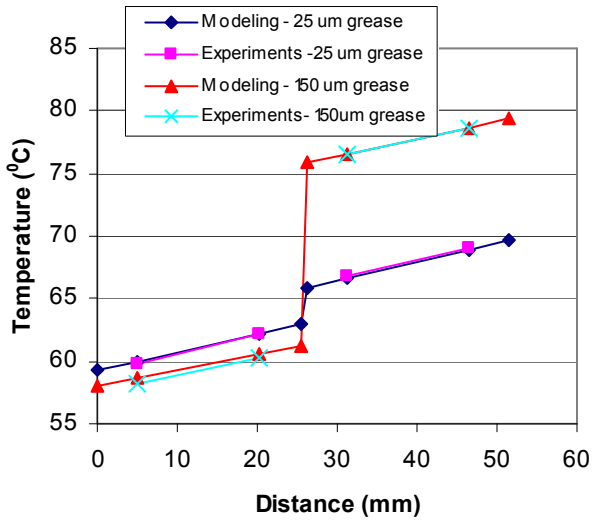

Fig. 6 Comparison of Experimental and Modeling Results

Test Results with Conventional Thermal Greases

In this section, we discuss experimental results for various commercially available greases. Greases are predominantly used in the automotive industry despite well-known problems related to pump-out and dry-out. The intent here is to understand the mechanisms underlying the thermal performance of greases and also to create a consistent, objective database against which to compare the performance of any alternative TIM.

Figure 6 shows a comparison of experimental and thermal modeling results with a conventional grease (Wacker Silicone P12). The average temperature in the metering blocks is plotted as function of the vertical distance, i.e., moving from the cold plate (0) to the hot plate (50.8 mm).

Results are shown for two different grease thicknesses: 25 and 150 microns. The step change in temperature at 25.4 mm is across the TIM. The modeling results indicate that the model is capturing the trend of the experimental results. Of course, in the modeling, there are a number of uncertainties, such as the heat loss coefficients on the boundaries and the contact resistance between the various layers in the apparatus. However, between the modeling results for the 25- and 150-micron grease layer cases, the only difference is the resistance of the interface material. This shows that the model is capturing the changes in the interface material quite well. In addition, the model shows that the experimental results are following the expected trends.

Since grease is still the most predominantly used interface material in the automotive power electronics industry, we performed experiments with some brands of commercially available thermal greases. Some of these greases (Aavid Thermalloy Thermalcote 251G, Wacker Silicone P12) are currently in use in automotive inverters. These experiments

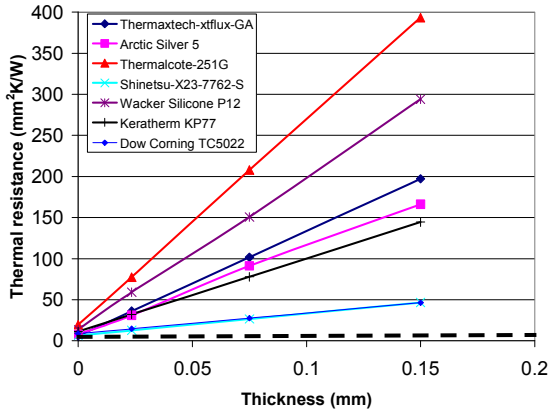

Fig. 7 Thermal Resistance vs. Thickness for Different Greases (dashed line: target value of 3 mm^2K/W)

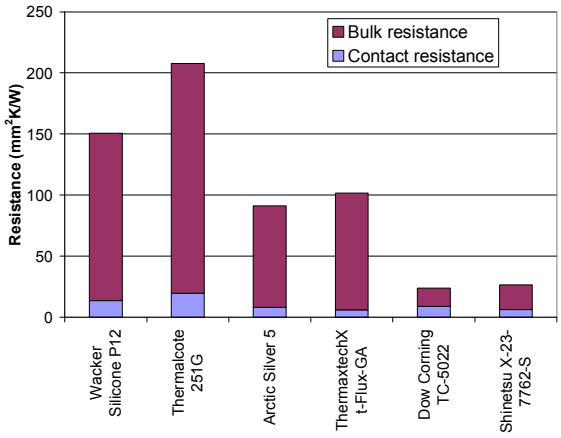

Fig. 8 Contribution of Bulk and Contact Resistances for Various Greases (at 75 microns BLT and an average sample temperature of ~75°C)

were performed over a sample temperature range of 55° to 80°C, a thickness range of 25 to 150 microns, and an applied pressure of 0.17 to 0.34 MPa. Figure 7 shows the thermal resistance as a function of grease thickness at an average sample temperature of ~75°C for the various greases. In the near future, trench IGBTs will soon be the norm. These trench IGBTs have a maximum temperature rating in the range of 150° to 175°C. Hence, it is important to characterize the performance of these greases at elevated temperatures of the order of 150°C. We plan to do this in the near future.

To maintain the thickness of the grease layer, we used glass spheres acquired from Mo Sci Corporation. The volume of the glass spheres is a negligible fraction of the total volume of the grease between the metering blocks. Figure 7 shows that, as the grease thickness increases, the thermal resistance also

increases linearly, as expected. For any given grease thickness, the thermal resistance may also change as a function of temperature. We found this change to be as much as 8%, in some cases, over a temperature range from 55° to 80°C. However, not all greases exhibited this behavior.

For any given grease listed in Figure 7, the inverse of the slope of the linear curve gives the thermal conductivity of the material, and the y-intercept gives an estimate of the contact resistance. From a thermal perspective, the Shinetsu-X23-7762-S and Dow Corning TC-5022 greases are high-performance materials. For a 25-micron thick layer, the thermal resistance is 13 and 15 mm^2K/W for Shinetsu and Dow Corning, respectively. Even for a 150-micron thick layer, the thermal resistance is only about 45 and 47 mm^2K/W for Shinetsu and Dow Corning, respectively. In our study, we are exploring a TIM thickness range of 25 to 150 microns, because in actual packages, manufacturing constraints may cause unavoidable gaps of 100 to 150 microns.

Figures 7 and 8, as well as Table 2, show contact resistances for the various greases. Individual differences in the greases may be a result of how well they wet the surfaces and fill up the microscopic surface irregularities [5]. The Shinetsu-X23-7762-S and Thermaxtech-Xtflux-GA greases have the lowest contact resistances. However, for all the greases, the contact resistances are in the range of 6 to 20 mm^2K/W. Though not presented in this paper, the contact resistance of TIMs can be estimated theoretically [3-5]. It would be interesting to compare modeling results for contact resistance with the experimental results obtained here. Arguably, the contact resistance of greases is quite low, which may be one reason for their widespread use despite significant drawbacks. Figure 8 shows that, as the BLT of the grease increases, the bulk resistance of the grease dominates over the contact resistance.

Table 2. Comparison of Various Greases as to Thermal Resistance, Conductivity, Composition, and Cost

Grease	**Thermal Resistance @ ~75°C (mm^2K/W)**				**Thermal Conductivity (W/mK)**		**Composition**	**Cost ($/g)**
	Contact Resistance (mm^2K/W)	**23.5 µm (Total resistance)**	**75 µm (Total resistance)**	**150 µm (Total resistance)**	**Expt. @~75° C**	**Mfg. Data**		
Wacker Silicone P12	**13.6**	**59.1**	**150.8**	**294**	**0.54**	**0.8**	Dimethylsil-oxane(s) with filler (trade secret)	0.07
Aavid Thermalloy Thermalcote 251 G	**19.6**	**77.5**	**207.9**	**393.3**	**0.4**	**0.39**	Polydimethyl-siloxane (30%-60%); zinc oxide (30%-60%)	0.04
Arctic Silver 5	**7.9**	**30.9**	**91.0**	**166.1**	**0.94**	**8.7**	Silver, boron nitride, zinc oxide, aluminum oxide, ester oil blend	2
Thermaxtech Xt-flux-GA	**6.0**	**36**	**101.6**	**197.2**	**0.78**	**7**	Silicone oil, high-purity particles (info. not available)	1.2
Dow Corning TC-5022	**8.7**	**16.7**	**23.8**	**47.8**	**4.0**	**4.0**	Dimethyl, methyldecyl-siloxane (1%-~5%), metal oxides, treated fillers (trade secret)	0.43
Shinetsu X-23-7762-S	**6.3**	**12.6**	**26.5**	**46.6**	**3.7**	**4.4**	Aluminum (>60%), zinc oxide (<30%), unknown solvent (trade secret)	0.9

Overall, the results in Figure 7 suggest that high-performance greases can yield resistances as low as 13 and 33 mm^2K/W, for a BLT of 25 and 100 microns, respectively. Our analysis indicates that the interface material completely stops being a bottleneck below a resistance of 3 mm^2K/W for a conventional

IGBT package configuration. The results here suggest that, while the commercially available greases tested in this study can be used to obtain very good performance, none approaches 3 mm^2K/W for practical BLTs. In addition, reliability is a concern with a majority of the greases. Aspects related to reliability include performance after thermal cycling (pump-out), aging effects (dry-out effects on viscosity, thermal performance), and uniform application.

Table 2 is a summary and comparison (including costs and chemical composition) of most of the greases that were tested. The cost numbers are given as $/gram of grease, but this number can be highly influenced by the quantity purchased. A typical IGBT package footprint in an inverter is about 13,560 mm^2. Assuming a grease thickness of 75 microns gives a total grease volume of about 1000 mm^3. Given that the density of the grease could vary from 1600 kg/m^3 (Thermalcote 251G) to 4100 kg/m^3 (Arctic Silver 5), the weight of grease required for a single inverter varies from 1.6 to 4.1 grams.

From the cost numbers in Table 2, this means that the cost of grease for a single inverter can vary from $0.06 to $8.40, depending on the type of grease used. Again, estimating costs can be very tricky, and some of the cost numbers provided in Table 2 could change drastically based on the quantity purchased (e.g., Arctic Silver 5 and Thermaxtech-Xtflux-GA).

The Wacker Silicone P12 ($0.16/inverter application) and Thermalcote 251G ($0.06/inverter) greases are certainly less expensive than the Shinetsu X23-7762-S ($2.25/inverter) or the Dow Corning TC-5022 ($1.40/inverter). However, the thermal performance of Thermalcote 251G and Wacker Silicone P12 is also considerably inferior to that of the Shinetsu or Dow Corning greases.

The key to the good performance of the Shinetsu grease seems to be a high content of very conductive particles and an unknown solvent that enhances performance. This solvent is considered to be a trade secret. The solvent evaporates over time (a few weeks or months), so the viscosity of the grease increases over time. As a consequence, the Shinetsu grease is not as easy to work with as the Thermalcote 251G and Wacker Silicone P12 greases. It is not clear how reliable the Shinetsu grease will be over time. We plan to characterize aspects related to the reliability of the TIMs in the near future.

Test Results for Phase-Change Materials and Thermoplastics

We also performed measurements on some PCMs and thermoplastics through both the steady-state and the transient laser flash approaches. Figure 9 shows the results for two phase-change materials (Honeywell PCM45-G and Loctite Powerstrate XtremePS-X) and two thermoplastics (Cookson Staystik 1172 and Btech TP-1).

The PCM changes phase (solid to liquid) at a temperature of the order of 50°C. The PCMs are placed between the two bounding layers, and the temperature of the PCM has to be about 50°C at least once in order for the PCM to change

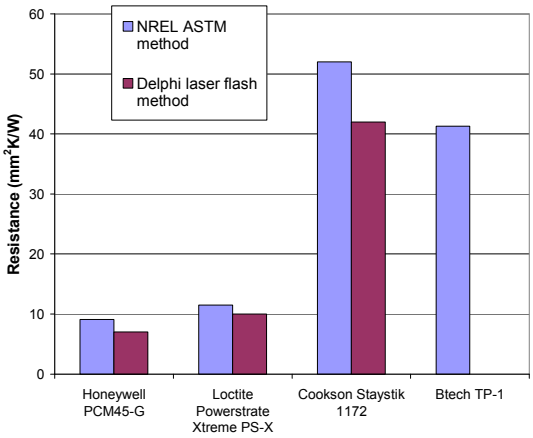

Fig. 9 Comparison of Steady-State and Transient Laser Flash Approaches for Thermal Resistance Measurement of PCMs and Thermoplastics

phase. Upon cooling, the PCM has adhesive properties and forms a bond between the two bounding layers.

Thermoplastics are also of interest in the automotive industry because, upon curing, they function as adhesives and hold the bounding layers of the package together without any external clamping mechanism. The curing process involves keeping the bounding layers and the thermoplastic at a temperature of 150°C under a pressure of 0.2 MPa for about half an hour, and then allowing the assembly to cool down to room temperature. For the results shown in Figure 9, the average sample temperature is about 62°C and the pressure is 0.17 MPa.

For the steady-state method, the TIM is placed between the two metering blocks (Figure 5). For the transient laser flash method, the TIM is placed between the aluminum and DBC-aluminum nitride layers. This aspect itself could cause some of the discrepancy in the results from both the steady-state and transient laser flash methods.

It is important to note that, unlike the experiments with greases, the BLT of the PCMs and thermoplastics was not controlled during the experiments. The lack of BLT control also is closer to a real-world application. For the PCMs, we found a reasonable match between the results (Figure 9) from the two approaches (within 20%); for the thermoplastics, however, there is noticeable discrepancy in the results (within 30%). For the thermoplastics, there is a difference in the processing conditions (curing process) for the tests with the two different approaches. Figure 9 shows that the PCMs have very low thermal resistances (~8-10 mm^2K/W); however, their reliability and suitability for automotive applications remains to be proven.

Some studies in the literature [5] indicate that the performance of a PCM degrades when it is exposed to elevated temperatures over a period of time. The environment in automotive power electronics is harsher than it is in computer microelectronics [5].

Figures 7, 8, and 9 gave an indication of the thermal resistance numbers associated with the various TIMs. It is worthwhile to explore the impact of these numbers on the maximum die temperature in a realistic power electronics package. We do this through the 3-D ANSYS finite element simulations presented earlier. The domain for the simulations remains the same as that in Figure 2. The results for temperature are again accurate (mesh-independent) to within 1%. Figure 10 shows the maximum IGBT junction temperature as a function of total TIM thermal resistance for each of the three grease thicknesses considered in this study (25, 75, and 150 microns). The lowest grease thermal resistance from Table 1 is 12.6 mm^{2}K/W; the highest is about 393.3 mm^{2}K/W. Figure 10 shows that the difference in the maximum IGBT temperature for the lowest and highest thermal resistance cases is almost 58°C, which is a significant difference.

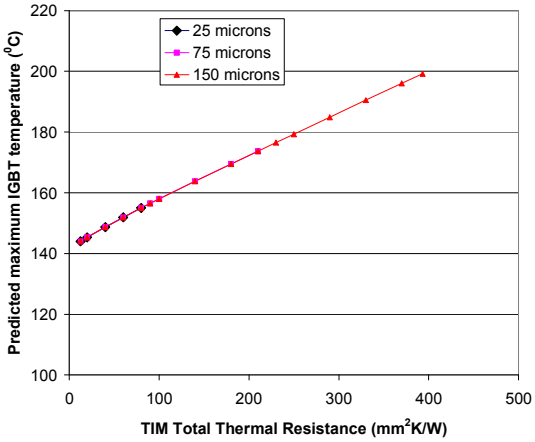

Fig. 10 Predicted Maximum IGBT Junction Temperature as a Function of the Total TIM Thermal Resistance for the Various Greases

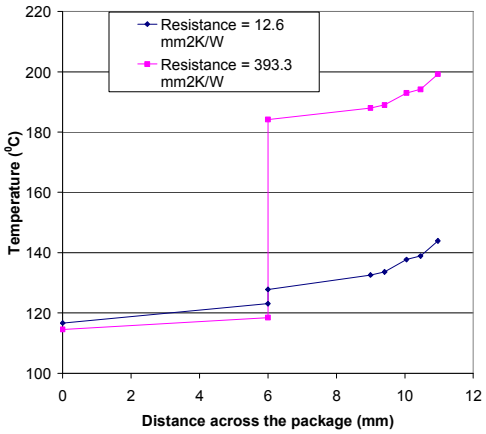

Fig. 11 Temperature Across the Cross Section of the IGBT Package (AA in Figure 2(C)) for Two Extremes of the TIM Resistance

Figure 11 shows the temperatures across a cross section (AA in Figure 2(c)) through the IGBT package for the Prius inverter for the two extremes in TIM thermal resistance (12.6 and 393 mm^{2}K/W). For a TIM resistance of 12.6 mm^{2}K/W, the temperature jump across the TIM is only 4.7°C. However, when the TIM resistance is 393 mm^{2}K/W, the temperature jump across the TIM is about 65°C. This suggests that, even within greases, one has to be careful of the type and thickness of grease that is applied, since this can have a significant impact on the die temperatures, as demonstrated in the results presented here.

CONCLUSIONS

This paper demonstrates that TIMs pose a significant bottleneck to heat removal from the IGBT package. From a DOE Vehicle Technologies Program and automotive industry perspective, a reliable, cost-effective, and high-thermal-performance TIM can help to meet some program goals. These goals could include cooling with 105°C glycol-water, or even air cooling, and extracting maximum heat flux from the device, whether it be conventional silicon-based, trench IGBT or silicon-carbide-based, and keeping the maximum temperature within acceptable limits.

We acquired, tested, redesigned, and improved a test stand based on the ASTM D5470 steady-state test method to make thermal resistance measurements of several TIMs. Experiments were performed with several conventional thermal greases, and their performance was characterized over a range of temperatures and BLTs. The Shinetsu and Dow Corning greases are superior in thermal performance over other greases that were tested. These results suggest that care has to be taken in choosing the type of grease and the thickness of the grease that is applied, since its impact on die temperatures is significant. Results also suggested that the contact resistance of greases is fairly low.

The results also indicated that none of the tested greases were able to go below a resistance of about 33 mm^{2}K/W at BLTs of 100 microns or greater. Practical inverter configurations are likely to require a TIM thickness of about 100 microns. Hence, a conservative goal would be to identify or fabricate a TIM that would have a thermal resistance of about 3 mm^{2}K/W at bond line thicknesses approaching 100 microns. The phase-change materials tested have a fairly low thermal resistance (~8-10 mm^{2}K/W), but it is likely that the BLT of PCMs during the experiments was fairly low (<25 microns). The match between the results from the ASTM steady-state method and those from the transient laser flash method is fair, given all the uncertainties involved.

In addition to the TIMs considered in this study, other TIMs (such as metallic TIMs, graphite, and CNTs) will also be studied. For materials with promising thermal performance, we plan to characterize all aspects related to reliability in the automotive environment. These include the impacts of thermal cycling and aging on the TIM thermal resistance. The impact of elevated temperatures (~150°C) on the performance of the TIMs will be explored. We also plan to characterize the automotive power electronics package in situ performance of the most promising TIMs.

ACKNOWLEDGMENTS

The authors would like to acknowledge the support provided by Susan Rogers, Technology Development Manager for Power Electronics and Electrical Machines, Vehicle Technologies Program, DOE Office of Energy Efficiency and Renewable Energy. The authors would also like to thank Keith Gawlik and the power electronics team at NREL for helpful discussions and interactions.

REFERENCES

[1] R.H. Staunton, L.D. Marlino, J.N. Chiasson, and T.A. Burress, "Evaluation of 2004 Toyota Prius Hybrid Electric Drive System," Oak Ridge National Laboratory Technical Report, ORNL/TM-2006/423, 2006.

[2] M. O'Keefe and K. Bennion, "A Comparison of Hybrid Electric Vehicle Power Electronics Cooling Options," IEEE Vehicle Power and Propulsion Conference, 2007.

[3] C.V. Madhusudana, *Thermal Contact Conductance*, New York: Springer-Verlag, 1996.

[4] M.M. Yovanovich and E.E. Marotta, "Thermal Spreading and Contact Resistances," in *Heat Transfer Handbook,* A. Bejan and A.D. Kraus, Editors, Hoboken, NJ: John Wiley & Sons, pp. 261−395, 2003.

[5] R. Prasher, "Thermal Interface Materials: Historical Perspective, Status and Future Directions," in *Proceedings of the IEEE*, Vol. 94, No. 8, pp. 1571–1586, 2006.

[6] B.A. Cola, J. Xu, C. Cheng, X. Xu, T.S. Fisher, and H. Hu, "Photoacoustic Characterization of Carbon Nanotube Array Thermal Interfaces," *Journal of Applied Physics*, Vol. 101, No. 054313, 2007.

[7] American Society for Testing and Materials, ASTM Standard D5470-01, 2005.

[8] S.V.J. Narumanchi, *Advanced Thermal Interface Materials to Reduce Thermal Resistance,* NREL Technical/Milestone Report No. TP-540-40617, 2006.

[9] R.C. Campbell, S.E. Smith, and R.L. Dietz, "Measurements of Adhesive Bondline Effective Thermal Conductivity and Thermal Resistance Using the Laser Flash Method," 15th IEEE Semitherm Symposium, pp. 83, 1999.

[10] H.J. Lee, "Thermal Diffusivity in Layered and Dispersed Composites," Ph.D. Thesis, Purdue University, University Microfilms International, 1975.

[11] S.J. Kline and F.A. McClintock, "Describing Uncertainties in Single-sample Experiments," *Mech. Eng.* (Am. Soc. Mech. Eng.), 75, pp. 3-8, 1953.

REPORT DOCUMENTATION PAGE

Form Approved
OMB No. 0704-0188

PLEASE DO NOT RETURN YOUR FORM TO THE ABOVE ORGANIZATION.

1. REPORT DATE *(DD-MM-YYYY)*	2. REPORT TYPE	3. DATES COVERED *(From - To)*
July 2008	Conference paper	

4. TITLE AND SUBTITLE
Thermal Interface Materials for Power Electronics Applications: Preprint

5a. CONTRACT NUMBER
DE-AC36-99-GO10337

5b. GRANT NUMBER

5c. PROGRAM ELEMENT NUMBER

6. AUTHOR(S)
S. Narumanchi, M. Mihalic, and K. Kelly: NREL;
G. Eesley: Delphi Electronics

5d. PROJECT NUMBER
NREL/CP-540-42972

5e. TASK NUMBER
FC087000

5f. WORK UNIT NUMBER

7. PERFORMING ORGANIZATION NAME(S) AND ADDRESS(ES)
National Renewable Energy Laboratory
1617 Cole Blvd.
Golden, CO 80401-3393

8. PERFORMING ORGANIZATION REPORT NUMBER
NREL/CP-540-42972

9. SPONSORING/MONITORING AGENCY NAME(S) AND ADDRESS(ES)

10. SPONSOR/MONITOR'S ACRONYM(S)
NREL

11. SPONSORING/MONITORING AGENCY REPORT NUMBER

12. DISTRIBUTION AVAILABILITY STATEMENT
National Technical Information Service
U.S. Department of Commerce
5285 Port Royal Road
Springfield, VA 22161

13. SUPPLEMENTARY NOTES

14. ABSTRACT *(Maximum 200 Words)*

In a typical power electronics package for a vehicle, a grease layer forms the interface between the direct bond copper layer or a baseplate and the heat sink. This grease layer has the highest thermal resistance of any layer in the package. Reducing the thermal resistance of the grease or other thermal interface material (TIM) can help to achieve Department of Energy FreedomCAR goals to use a glycol water mixture at 105 deg. C or even air cooling. This paper describes progress in characterizing the thermal performance of some conventional and novel TIMs. Experimental results for thermal resistance, in the context of automotive power electronics cooling, indicate that the thermal resistance of the TIM layer has a dramatic effect on maximum temperature in the power electronics package.

15. SUBJECT TERMS
hybrid electric vehicles; inverters; IGBTs; heat transfer; oscillating jets; vehicle power electronics

16. SECURITY CLASSIFICATION OF:			17. LIMITATION OF ABSTRACT	18. NUMBER OF PAGES	19a. NAME OF RESPONSIBLE PERSON
a. REPORT	b. ABSTRACT	c. THIS PAGE			19b. TELEPHONE NUMBER (*Include area code*)
Unclassified	Unclassified	Unclassified	UL		

Standard Form 298 (Rev. 8/98)
Prescribed by ANSI Std. Z39.18